Determination of surface heterogeneity of D-mannitol by sessile drop contact angle and finite concentration inverse gas chromatography

Raimundo Ho[a], Steven J. Hinder[b], John F. Watts[b], Sarah E. Dilworth[c], Daryl R. Williams[a], Jerry Y.Y. Heng[a,*]

[a] Surfaces and Particle Engineering Laboratory, Department of Chemical Engineering, Imperial College London, South Kensington Campus, London SW7 2AZ, UK
[b] The Surface Analysis Laboratory, Faculty of Engineering & Physical Sciences, University of Surrey, Guildford, Surrey GU2 7XH, UK
[c] Pharmaceutical and Analytical R&D, AstraZeneca, Macclesfield, Cheshire SK10 2NA, UK

A B S T R A C T

The sensitivity of two techniques in tracking changes in surface energetics was investigated for a crystalline excipient, D-mannitol. Macroscopic crystals of D-mannitol were grown from saturated water solution by slow cooling, and sessile drop contact angle was employed to measure the anisotropic surface energy. The facet-specific surface energy was consistent with localised hydroxyl group concentrations determined by X-ray photoelectron spectroscopy (XPS), and was also in excellent agreement with the surface energy distribution of the powder form of mannitol measured via a new methodology using inverse gas chromatography (IGC) at finite concentrations. The γ_{SV}^d was found to vary between 39.5 mJ/m^2 and 44.1 mJ/m^2 for contact angle and between 40 mJ/m^2 and 49 mJ/m^2 for IGC measurements. We report here, a high level of surface heterogeneity on the native mannitol crystal surfaces. When the surfaces of both D-mannitol samples (powder and large single crystals) were modified by dichlorodimethylsilane to induce surface hydrophobicity, both IGC and contact angle revealed a homogeneous surface due to functionalisation of mannitol crystal surface with methyl groups resulting in γ_{SV}^d of ~34 mJ/m^2. It was shown that both IGC and contact angle techniques are able to detect surface chemical variations and detailed surface energetic distribution.

1. Introduction

The pharmaceutical industry and regulatory authorities have traditionally directed their attention mainly to the quality and processability of active pharmaceutical ingredients (APIs), despite the notion that properties of solid-state pharmaceutical *excipients* can be reflected in various physicochemical parameters as well as in the processing behaviour and rate of release of the active ingredient (Pifferi et al., 1999). One important physicochemical property of solid-state pharmaceutical excipients is the surface free energy which governs interfacial interactions. Knowledge of surface energetics of excipients can therefore be of similar importance to that of the APIs in the formulation design of multi-component systems and the prediction of processing performance such as binder–drug adhesion (Begat et al., 2004), powder flow, compaction (Li et al., 2004) and granulation performances (Zhang et al., 2002; Thielmann et al., 2008). Common methods of characterising the surface energetics of particulate pharmaceuticals rely on indirect approaches

involving the use of characterised or *known* vapours, liquids or solids as probes as in inverse gas chromatography (IGC) (Newell et al., 2001), sessile drop contact angle (Heng and Williams, 2006) and atomic force microscopy (AFM) (Davies et al., 2005) respectively.

Amongst all liquid probe techniques, contact angle is one of the most commonly used techniques in the characterisation of surface energetics and wettability of pharmaceutical solids. Surface free energy of a solid may be estimated by measuring the contact angles of a series of known reference liquids on the surface using the classical Young's equation which was derived from a force balance acting at the three-phase contact point:

$$\gamma_{SV}^0 = \gamma_{SL} + \gamma_{LV} \cos\theta_Y$$

where γ_{SV}^0 is the surface energy of the solid free of an adsorbed vapour film, γ_{LV} is the liquid–vapour surface tension, γ_{SL} is the solid–liquid surface energy, and θ_Y is the Young contact angle. Measurements of contact angle can be performed on compressed powder surfaces, powder adhered to a glass slide or Wilhelmy plate methods on compressed plates, but these methods have significant limitations in the accurate assessment of surface energy (Buckton and Gill, 2007). An alternative approach is to conduct sessile drop contact angle measurements on surfaces of macro-

scopic crystals to derive surface energetic information (Heng et al., 2006a,b,c). Using macroscopic crystals, Heng et al. (2006a,b,c) were able to measure experimentally the anisotropic surface energetics and wettability of APIs. The facet-specific surface energetics were found to be mainly due to the chemical heterogeneities present on the surfaces, with negligible influence on the data due to surface roughness, dissolution, swelling and non-equilibrium effects. The approach greatly enhances the quality and quantity of surface energetic and chemical informations one can obtain from crystalline pharmaceuticals using a liquid probe technique such as contact angle.

IGC, the inverse use of gas chromatography, is a versatile vapour probe technique which is applicable to powders and fibrous materials, and compatible with sample porosity, irregular surface topographies and surface inhomogeneity. Experiments in IGC are conducted by packing the solid sample of interest in a column and then injecting *known* vapour probes into the column via an inert carrier gas to probe the physiochemical properties of the sample. The determination of the dispersive surface energy, γ_{SV}^d, and acid–base adsorption energy, ΔG_{AB}^0, as well as the basic and acidic properties of the solid samples are well documented (Heng et al., 2006a,b,c; Buckton and Gill, 2007). The usual procedure of measuring surface energies by IGC is at infinite dilution where very small concentrations of probe vapours ($<0.03\, p/p_0$) are injected. These small concentrations of adsorbates are thought to preferentially interact with the higher energy sites on the material surface and the interaction with lower energy sites of the adsorbent would be limited, if not excluded (Newell and Buckton, 2004). Therefore, the measured energy may be higher than that measured from contact angle when the energy is expressed as an average of the probed area or surface sites.

A fundamental feature of real solid surfaces is surface heterogeneity which may be due to presence of impurities, different crystal facets, growth steps, crystal edges, surface pores, local degree of crystallinity and surface functional groups. An important aspect of IGC is its ability to estimate surface energetic heterogeneity based on pressure or temperature dependence methods, and details of these methodologies can be found elsewhere (Jaroniec and Madey, 1988; Charmas and Leboda, 2000). However, these previously used methods suffer from the fact that they are probe molecule dependent, because the interactions of the adsorbing molecules with surface sites depend on the chemical nature of the adsorbates, thus only provide information concerning the 'relative' heterogeneity which can only be used as fingerprints for comparisons between different materials. A new approach recently developed by Thielmann et al. (2007) permits the characterisation of the *explicit* γ_{SV}^d distribution of particulate materials from the adsorption isotherms of a series of n-alkanes using IGC at finite concentration conditions using pulse injection method. The methodology was applied to measure differences in γ_{SV}^d and ΔG_{AB}^0 (ethanol) distribution profiles of untreated, amorphous and recrystallised lactose. Their results showed that recrystallised lactose sample is energetically more homogenous than milled and untreated samples due to surface amorphous regions and anomeric composition respectively (Thielmann et al., 2007). This surface energy heterogeneity method has also applied in the characterisation of ibuprofen racemate crystals (Ho et al., 2008).

D-mannitol ($C_6H_{14}O_6$), an hexa-hydric sugar alcohol, is the subject crystalline pharmaceutical excipient investigated in the current study. Due to its desirable physicochemical properties such as its non-hygroscopicity, non-cariogenicity and cooling property in the oral cavity, D-mannitol is commonly used in a variety of formulations as in oral and chewable tablets, powder granules and moisture sensitive APIs (Yoshinari et al., 2002). Three polymorphic forms were identified for D-mannitol: a thermodynamically stable orthorhombic β form, a less stable orthorhombic α form and a very

unstable monoclinic δ form (following the nomenclature of Walter-Levy, 1968). The orthorhombic β form is most commonly used in the pharmaceutical industry due to its thermodynamic stability at ambient conditions, though δ form was shown to possess better tabletting properties (Burger et al., 2000). Despite its widespread use in pharmaceutical formulations, detailed reports on its surface energetic properties are limited. Saxena et al. (2007) applied molecular modelling method to predict the surface energies of individual facets of D-mannitol crystals by evaluating the interaction energies between individual atoms of adsorbating molecules and atoms of the molecule orientated on the specific surface. The reported γ_{SV}^d of facet $(0\,2\,0)$ and $(1\,\bar{1}\,0)$ were 56.2 mJ/m² and 55.3 mJ/m² respectively, without observable difference between the two crystal planes. These γ_{SV}^d values were, however, significantly higher than the value measured by Grimsey et al. (1999) using IGC at infinite dilution at 47.9 mJ/m². Although molecular modelling provides a mean to elucidate the effects of surface chemistries and molecular orientations on surface energetics, reliability of the surface energy data obtained are limited to the assumptions in the methodology used to model the interactions between the probing molecules and the surface under consideration, without accounting for influence due to surface physical conditions, e.g. presence of impurities and adsorbed molecules, amorphous regions, topography, etc. as well as temperature effects.

In the current study, the surface energetics of D-mannitol were determined via contact angle measurements on single macroscopic crystals, and by IGC at finite concentration to obtain surface energy distribution as aforementioned. Sessile drop contact angle and IGC surface energy hetereogeneity measurements are complimentary techniques in determining detailed surface energetics. In an attempt to illustrate and prove the validity of these complimentary techniques in detecting surface chemical changes, D-mannitol was also subjected to surface silanisation with methylene groups to promote change in surface chemistry, therefore energetic heterogeneity. The influence of surface chemistry in high shear granulation behaviour and granule attributes is the subject of separate paper currently in preparation.

2. Materials and methods

2.1. Macroscopic crystallisation of D-mannitol

β D-Mannitol seed crystals of a few millimeters in size were obtained by recrystallising a supersaturated solution of D-mannitol (Ph Eur Pearlitol® 160C, Roquette, France) in analytical grade deionised water at room temperature. To obtain macroscopic crystals with large and distinguishable facets, a single seed crystal was tied with a single aramid fibre (diameter = 10 μm), suspended in a saturated solution of D-mannitol in water at 30 °C without stirring and allowed to cool slowly to 15 °C at a rate of 1 °C/day. Reseeding the crystal in fresh solution at 30 °C was required to obtain crystal of macroscopic (>1 cm) scale. 1% (w/v) of isopropanol (99.6%, Acros Organics, Geel, Belgium) was added to the solution to improve the crystal clarity and prevent bacterial growth. The habit of macroscopic single crystals obtained is shown in Fig. 1. The crystal habit corresponds to that reported in the literature (Kaminsky and Glazer, 1997), with major indexed facets $(1\,2\,0)$, $(0\,1\,1)$ and $(0\,1\,0)$. However, facets $(2\,1\,0)$ and $(1\,1\,0)$ were absent after long growth period. The crystals were dried under ambient conditions prior to contact angle measurements or surface chemical treatments.

The crystal structure of D-mannitol of the polymorphic form β was refined by Kaminsky and Glazer (1997) with a R-value of 0.0276. β D-Mannitol crystallises in the orthorhombic form with four ($z = 4$) molecules in each unit cell and of $P2_12_12_1$ space group. The unit cell parameters, obtained from Cambridge Structural
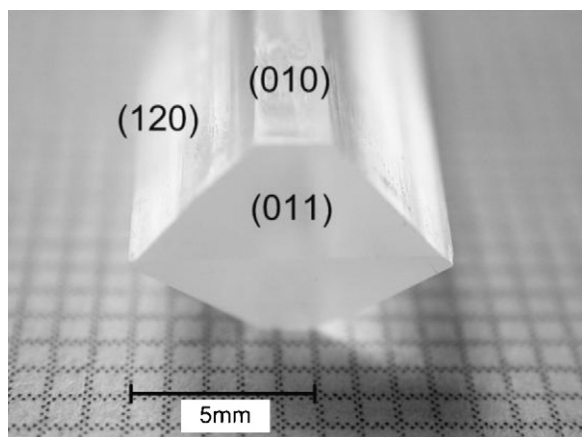
Fig. 1. Macroscopic crystals of β D-mannitol grown from aqueous solution.

Database (CSD) (Cambridge Crystallographic Data Centre, Cambridge, U.K.), are as follows: $a = 8.694$ Å, $b = 16.902$ Å and $c = 5.549$ Å (CSD Refcode: DMANTL07). Mercury (version 1.4.2, Cambridge Crystallographic Data Centre, Cambridge, U.K.) was used to visualise the crystal structure.

2.2. Surface modification

Surfaces of macroscopic crystals and untreated powder of D-mannitol were methylated by mixing the respective samples in separate solutions of 5% (v/v) dichlorodimethylsilane (≥99.5% Aldrich, Poole, U.K.) in trichloroethylene (≥99.5% Sigma–Aldrich, Poole, U.K.) at 80 °C for 3 h under constant reflux, according to the reaction pathway as shown in Fig. 2. The mixtures were agitated continuously during the reaction process to ensure good dispersion and methylation of surface hydroxyl groups. The liquid was decanted off after reaction and the samples were dried in a vacuum oven at 80 °C for 2 h. Materials were stored at 4 °C before characterisation.

2.3. Contact angle measurements

Sessile drop contact angles were obtained with a Krüss drop shape analyser (DSA 10, Krüss GmbH, Hamburg, Germany) with analytical grade deionised water, diiodomethane (>99%, Acros Organics, Geel, Belgium) and saturated aqueous D-mannitol solution as probe liquids. The saturated solution was prepared by stirring D-mannitol powder in analytical grade deionised water at 20 °C until the powder no longer dissolved. Initial drops of ~5 μL were dispensed onto the solid crystal facet. Advancing contact angles, θ_A, were measured by continual addition of the test liquid onto the droplet using a motor-driven syringe, and receding contact angles, θ_R, were obtained by removal of the test liquid. The needle tip was immersed and remained within the top half of the droplet which was monitored with a CCD camera. Contact angles were determined using the Drop Shape Analysis software (DSA version 1.0, Krüss GmbH, Hamburg, Germany). A minimum of 15 droplets on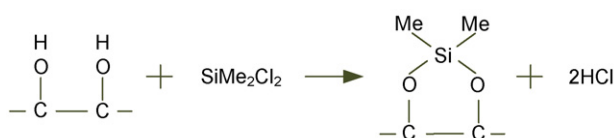 more than 5 single crystals were measured on each crystal facet. Experiments were conducted at a temperature of 20 ± 2 °C.

2.4. Inverse gas chromatography

IGC experiments were conducted using an iGC 2000 (Surface Measurement Systems, London, U.K.) with a flame ionisation detector. Untreated and surface modified D-mannitol powders from 75 μm to 180 μm sieve cut (representative of the majority of the sample particle size), were packed into separate standard pre-silanised columns (300 mm × 4 mm ID) with silanised glass wool at each end to prevent powder bed movement. Columns were filled with ~2 g of material and then conditioned in situ in the iGC with helium purge at 20 sccm for 2 h at 303 K to remove physisorbed water. Following pre-treatment, pulse injections using a 0.25 mL gas loop at 303 K were performed. A series of purely dispersive n-alkane vapour probes (decane, nonane, octane, heptane) (HPLC grade, Sigma–Aldrich, Poole, U.K.) were injected at $0.03 \, p/p_0$, $0.05 \, p/p_0$, $0.10 \, p/p_0$, $0.25 \, p/p_0$, $0.50 \, p/p_0$, $0.60 \, p/p_0$, $0.70 \, p/p_0$, $0.80 \, p/p_0$ and $0.95 \, p/p_0$ to determine the adsorption isotherms, and net retention volumes, V_N, were determined using peak maximum analysis as described in Thielmann et al. (2007). Ethanol (99.7–100%, v/v, Merck KGaA, Darmstadt, Germany) was injected at the same series of concentrations to determine non-dispersive interactions. Methane gas was injected at $0.10 \, p/p_0$ to determine column dead time. Helium, at a flow rate of 10 sccm, was used as the carrier gas for all injections. V_N and adsorption isotherms were calculated using SMS-iGC Analysis Macros (version 1.2, Surface Measurement Systems, London, U.K.). BET surface area was determined by standard nitrogen adsorption technique (Tristar 3000, Micromeritics, Norcross, GA).

2.5. X-ray photoelectron spectroscopy (XPS)

XPS spectra were acquired on all available facets of macroscopic D-mannitol crystal using a Sigma Probe spectrometer (Thermo VG Scientific, East Grinstead, U.K.). The instrument is equipped with both a microfocus monochromated AlKα source and a standard twin anode source (AlKα/MgKα). In this work, the twin anode AlKα X-ray source ($h\nu = 1486.6$ eV) was used at 300 W (15 kV × 20 mA). For all survey spectra, the pass energy was set at 100 eV. The pass energy was set at 20 eV for C 1s and O 1s high resolution, core level spectra. The samples were held in place on the instruments sample stage by sprung Cu/Be clips. Quantitative surface chemical analyses were calculated from the high resolution, core level spectra following the removal of a non-linear (Shirley) background. Fitting was performed using the manufacturers Advantage software (version 2.0.35, Thermo VG Scientific, East Grinstead, U.K.) which incorporates the appropriate sensitivity factors and corrects for the electron energy analyzer transmission function.

2.6. Polymorph identification

X-ray powder diffraction spectra were obtained for the silanised and untreated powder samples using a X'Pert Pro diffractometer (PANalytical B.V., Almelo, The Netherlands) over the range of 10–50° 2θ with a CuKα X-ray source at 40 kV and 40 mA.

3. Results and discussion

3.1. Contact angle analysis of D-mannitol single crystals

θ_A and θ_R were measured on all available facets of macroscopic single D-mannitol crystals with diiodomethane and water, presented in Table 1 (standard deviation $n \geq 15$ measurements). For characterisation of pharmaceutical crystals, θ_A were used to

Fig. 2. Chemical reaction of surface hydroxyl groups of D-mannitol (Me denotes a methyl group).

Table 1
θ_A, θ_R and $\Delta\theta$ (°) for specific crystalline facets of untreated D-mannitol and silanised D-mannitol crystal.

	Facet	(0 1 0)	(1 2 0)	(0 1 1)
Untreated D-mannitol				
Diidomethane	θ_A	30.3 ± 2.4	31.9 ± 2.9	40.1 ± 1.5
	θ_R	–	16.3 ± 2.7	15.2 ± 2.7
	$\Delta\theta$	–	15.6	24.9
Water	θ_A	56.2 ± 1.9	46.2 ± 2.2	12.8 ± 4.6
	θ_R	–	15.0 ± 3.6	–
	$\Delta\theta$	–	31.2	–
Mannitol–saturated water	θ_A	59.7 ± 9.5	48.1 ± 4.9	16.8 ± 6.2
	θ_R	–	27.7 ± 4.3	–
	$\Delta\theta$	–	20.4	–
Silanised D-mannitol				
Diidomethane	θ_A	48.8 ± 2.1	49.4 ± 2.4	48.8 ± 2.2

approximate θ_Y as in previous studies (Heng et al., 2006a,b,c; Ho et al., 2008). θ_A for diiodomethane on facets (0 1 0) and (1 2 0) was found to be very similar at about 30°, whereas that on facet (0 1 1) was approximately 40°, about 30% higher. θ_A of diiodomethane indicated that similar long-range dispersive interactions are present on facet (0 1 0) and (1 2 0), whereas facet (0 1 1) possesses weaker van der Waals dispersive interactions. On the basis of for diiodomethane, an order of the van der Waals type θ_A of interactions for β D-mannitol facets can be proposed:

$$(0\,1\,0) \approx (1\,2\,0) > (0\,1\,1)$$

The hydrophilicity of the three facets of D-mannitol was determined from θ_A for water. Surfaces which exhibit low θ_A for water are considered hydrophilic whilst high θ_A indicates hydrophobic propensity. The highest θ_A of water was obtained on facet (0 1 0) whereas facet (0 1 1) was almost fully wettable with water, i.e. $\theta_A < 10°$. The major problem with measuring θ_A on D-mannitol with water is crystal dissolution, as D-mannitol has a relatively high solubility in water; at 20 °C, the saturation concentration is 182 g/L (Kaminsky and Glazer, 1997). To establish the significance of dissolution on the contact angles measured, θ_A were also obtained with mannitol-saturated aqueous solution at the same experimental temperature of 20 ± 2 °C. As shown in Table 1, the measured values of θ_A were almost the same, within experimental error, for both water and mannitol-saturated water solution, and the rank order of wettability for the facets was identical. From the θ_A for water, the hydrophilicity order for β D-mannitol facets is:

$$(0\,1\,1) > (1\,2\,0) > (0\,1\,0)$$

A difference in θ_R and θ_A implies the occurrence of hysteresis. Despite extensive research, the reasons for the occurrence of con-

tact angle hysteresis have remained inconclusive. Some established phenomena that can cause contact angle hysteresis are surface roughness, chemical heterogeneity, material swelling, dissolution, surface restructuring and other non-equilibrium effects. The contact angle hysteresis showed in Table 1 was in the range of 15–32°, suggesting that non-ideal wetting of the surfaces due to thermodynamic or kinetic effects was relatively insignificant. In the current study, no swelling of crystals occurred with the probe liquids used, and no time-dependent contact angle effects were observed. The θ_A was used for calculation of surface energetics as commonly reported in literature.

The anisoptropic wettability of D-mannitol can be attributed to the variation in the concentration of surface functional groups on the individual facets. A simple estimation of the potential contributions of hydroxyl groups to the surface chemistry of the individual facet was obtained by determining density of 'free' hydroxyl groups which are liable to hydrogen bonding or polar interactions at each facet from accessing the number of exposed 'free' hydroxyl groups per unit cell surface area using Mercury software. Crystallographic structures at facets (0 1 0), (0 1 1) and (1 2 0), generated from crystal structure obtained from CSD using Mercury, are displayed in Fig. 3, and the estimated density of 'free' hydroxyl groups are summarised in Table 2. The increase in –OH group density correlates well with the order of hydrophilicity derived from contact angle data for both water and mannitol-saturated aqueous solution.

3.2. Crystal surface chemistry by XPS

Crystal surface chemistry was quantitatively determined by XPS from C 1s and O 1s XPS spectra for the crystal facets as shown in Fig. 4. Both the O 1s and C 1s spectra of all facets were similar; the O 1s spectra contain one main peak centered at ~533 eV binding
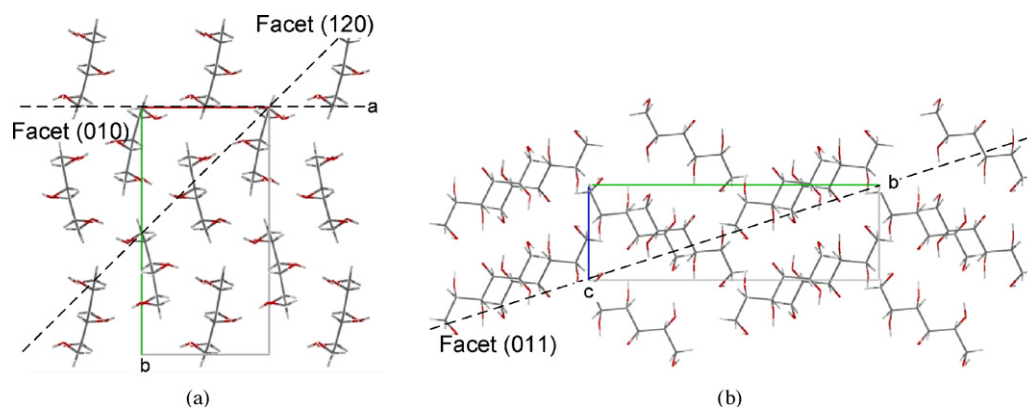

Fig. 3. Crystallographic structure of D-manntiol viewed along (a) c-axis and (b) a-axis.

Table 2
Unit cell information for D-mannitol and predicted free hydroxyl group surface concentrations.

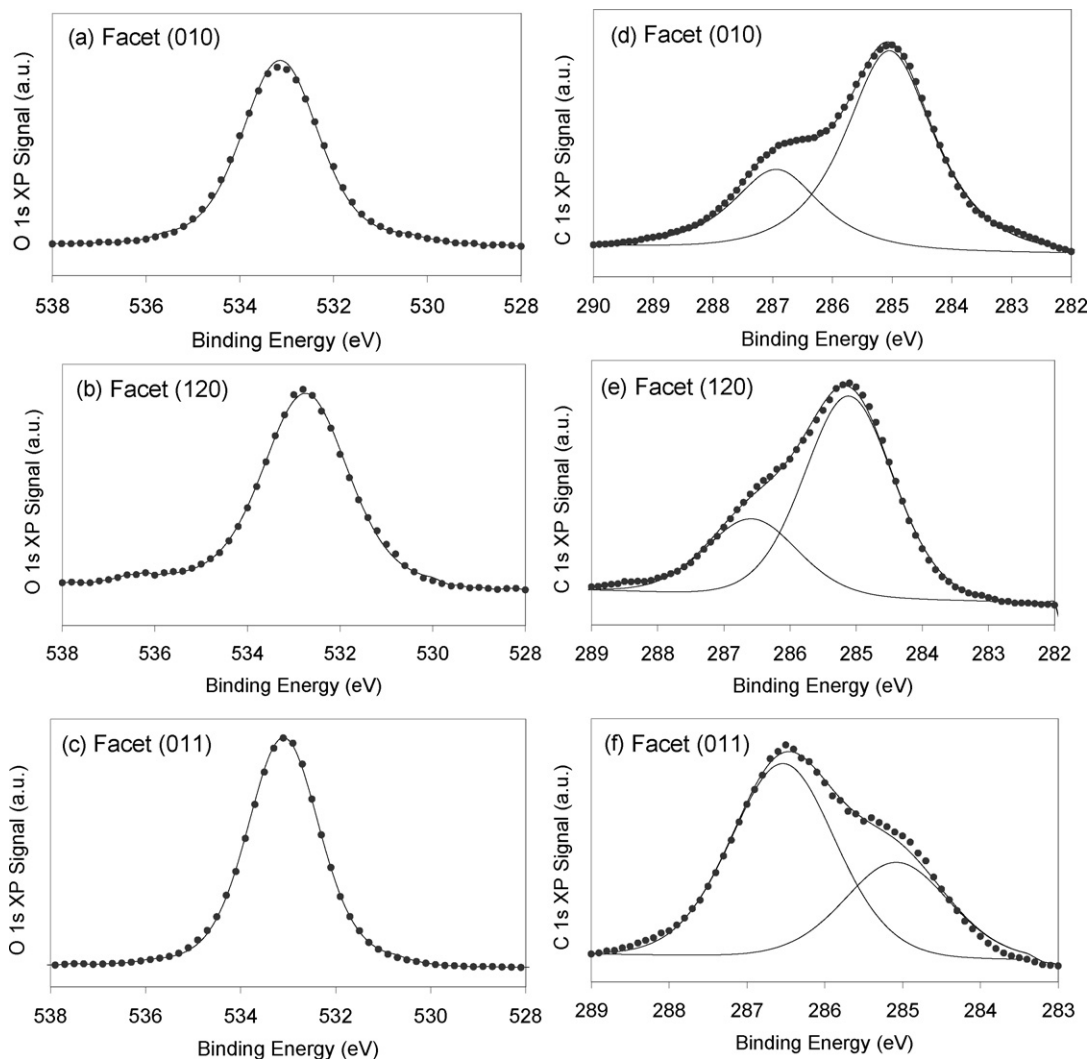| Facet	Unit cell length (Å)	Unit cell depth (Å)	Unit cell area (Å^2)	Approximate number of free OH groups	OH group density (Å^{-2})
(0 1 0)	8.694	5.549	48.24	2	0.0415
(1 2 0)	12.124	5.549	67.27	4	0.0595
(0 1 1)	17.789	8.694	154.66	11	0.0711

Fig. 4. O 1s XP spectra of (a) facet (0 1 0) (b) facet (1 2 0) and (c) facet (0 1 1) and C 1s XP spectra of (d) facet (0 1 0) (e) facet (1 2 0) and (f) facet (0 1 1) showing the deconvoluted C environments. FWHM of 1.92 eV and 1.65 eV were employed for all O and C 1s components respectively.

energies whereas C 1s spectra contain two peaks centered at 285 eV and 286.5 eV. The two unique C 1s chemical environments at 285 eV and 286.6 eV, revealed by deconvolution and peak fitting of the C 1s spectra, correspond to the CH$_x$ and alcohol (C–OH) functionalities respectively which are in excellent agreement with the molecular structure of D-mannitol. The presence of only one unique chemical environment at 532.9 eV in the O 1s spectra confirms that these facets expose only in acidic hydroxyl functionality.

Although the deconvoluted C 1s spectra reveal two unique carbon environments corresponding to apolar (CH$_x$) and polar (C–OH) carbons, the ratio of the polar to apolar carbon differs by more than 5 times on facet (0 1 1) compared to (1 2 0) and (0 1 0) as shown in Fig. 5. The surface composition also reveals that the (0 1 1) surface is the most oxygen rich whilst (0 1 0) is the least oxygen rich. The atomic percentage of oxygen for facet (0 1 1), (1 2 0) and (0 1 0) is 36.1%, 25.5% and 24.6% respectively, which is in excellent agreement with the order of hydrophilicity from θ_A for water and
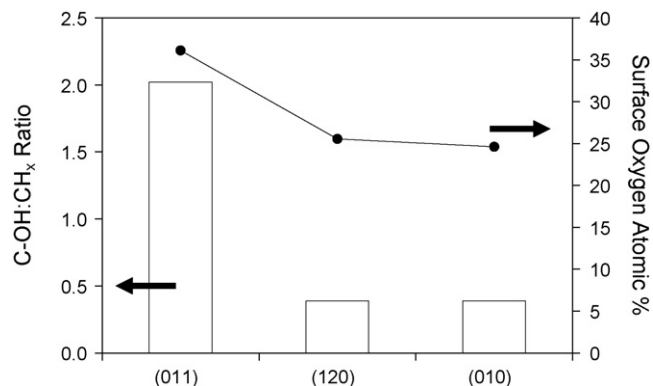

Fig. 5. Ratio of surface polar carbon to non-polar carbon for different facets of D-mannitol crystals as determined from the C 1s XP spectra and the corresponding surface atomic % of oxygen.
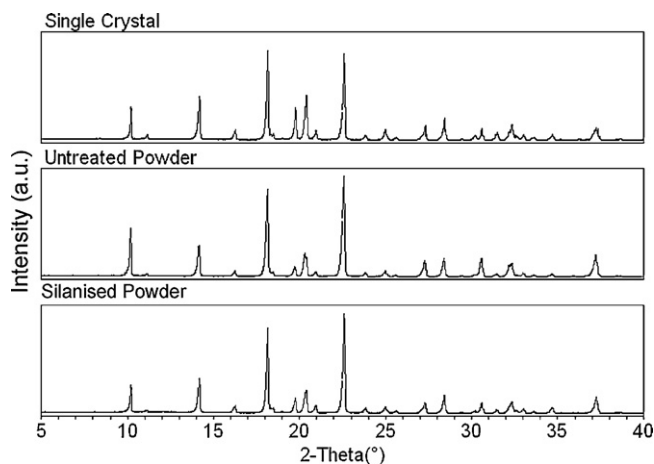
Fig. 6. X-ray powder diffraction patterns of single macroscopic crystal, untreated and silanised D-mannitol.

the estimated density of 'free' hydroxyl groups from the crystallographic structure. Both the C 1s and O 1s XP spectra confirms the presence of a higher concentration of hydroxyl functionalities on the (0 1 1) surface, and therefore this facet can be expected to be more polar and acidic. In contrast, the (0 1 0) facet exposes fewer polar hydroxyl functions resulting in a reduced potential for hydrogen bonding interactions.

3.3. Effects of surface methylation on contact angles

θ_A data for diiodomethane measured on silanised macroscopic D-mannitol crystals, displayed in Table 1, shows remarkable contrast to the anisotropic wettability on the untreated crystals. θ_A for diiodomethane were almost identical across all three facets at approximately 49°. The only difference between the untreated and silanised D-mannitol is that abundance of hydroxyl groups could be found on surfaces of the former whereas these –OH groups were substituted with –Si(CH$_3$)$_2$ groups on surfaces of the latter. The change from anisotropic wettability to an isotropic one as seen here can, therefore, be solely attributed to the change in surface chemistry, i.e. the surfaces became energetically homogeneous upon silanisation with methyl groups. To confirm that no polymorphic or crystallinity transition occurred as a result of the silanisation reaction, X-ray powder diffraction spectra was obtained on both the macroscopic crystal and powder samples (Fig. 6). The X-ray diffraction patterns of all silanised and untreated samples were compared to the theoretical patterns generated using single crystal data (Kaminsky and Glazer, 1997), and both samples were identified as β polymorph. Hence, the observed change in surface energetics was not due to undesired changes in molecular arrangements in the crystal lattice itself, but purely due to surface chemistry induced by silanisation.

3.4. Facet-specific surface energy from contact angle

Surface energy data were calculated using the classical Owens–Wendt methodology (Owens and Wendt, 1969) for dispersive, γ_{SV}^d, and polar, γ_{SV}^p, surface energy components using θ_A for diiodomethane and water. The calculated results are summarised in Table 3 for both untreated and silanised D-mannitol single crystals (significant differences from statistical analysis of the data). In the case of untreated D-mannitol, γ_{SV}^d and γ_{SV}^p depend on the specific facet being examined. This result reveals, the first time in an experimental perspective, that crystalline *excipient* like D-mannitol exhibits anisotropic surface energetics in a similar way to crystalline APIs. γ_{SV}^d of facet (0 1 0) is very similar to (1 2 0) whilst facet

Table 3
Surface energy (mJ/m^2) for untreated D-mannitol and silanised D-mannitol using the classical Owens–Wendt approach.

Facet	Untreated			Silanised	
	γ_{SV}^d	γ_{SV}^p	γ_{SV}	$\gamma_{SV}^p/\gamma_{SV}$	γ_{SV}^d
(0 1 0)	44.1 ± 0.6	12.8 ± 0.3	56.9 ± 0.9	0.23	34.9
(1 2 0)	43.3 ± 0.7	18.6 ± 0.4	61.9 ± 1.1	0.30	34.5
(0 1 1)	39.5 ± 0.4	35.4 ± 0.7	75.9 ± 1.0	0.47	34.9

(0 1 1) exhibits the lowest γ_{SV}^d. Conversely, γ_{SV}^p of facet (0 1 1) is the highest whilst facet (0 1 0) and (1 2 0) exhibit similar γ_{SV}^p. Grimsey et al. (1999) reported that the facet (0 1 0) is the predominant slip plane with the lowest attachment energy calculated from computational method. This result is consistent with our observations that the preferred cleavage plane is always the most hydrophobic facet, i.e. facet (0 1 0) in the case of β D-mannitol. Upon silanising the crystal, the heterogeneity in γ_{SV}^d disappeared (Table 3). The value of γ_{SV}^d across various indexed facets was almost identical at approximately 35 mJ/m^2, confirming their homogeneity in surface chemistry. The value of γ_{SV}^d was in excellent agreement with the γ_{SV}^d of polyethylene surface which exhibits similar surface chemistry (Owens and Wendt, 1969).

3.5. Surface energy distributions from IGC

Distribution of surface energetic properties is obtained in IGC by increasing the probe vapour partial pressure to finite concentration conditions such that a much greater number of surface sites is probed. The numerical determination of energy distribution of the sample is via a plot of V_N as a function of surface coverage, which is determined from the adsorption isotherm of the corresponding probe vapour. γ_{SV}^d or ΔG_{AB}^0 of the sample are then determined at a range of isosteres as opposed to a single injection concentration (typically 0.03 p/p_0) as in the infinite dilution conditions. A description of the methodology is detailed elsewhere (Thielmann et al., 2007).

A comparison of the relationship between V_N and surface coverage for all alkane probes are shown in Figs. 7 and 8 respectively for untreated D-mannitol and silanised D-mannitol. As a heterogeneous crystalline excipient, the retention volume of D-mannitol decreased with increasing surface coverage, because the interaction between the alkane probes and less energetic sites at high surface coverage would be weaker. For surface silanised D-mannitol, this trend in retention volumes disappeared, suggesting that the surface was energetically homogeneous. To obtain surface energy profile, γ_{SV}^d was calculated at different surface coverage following the methodology described by Schultz et al. (1987) in
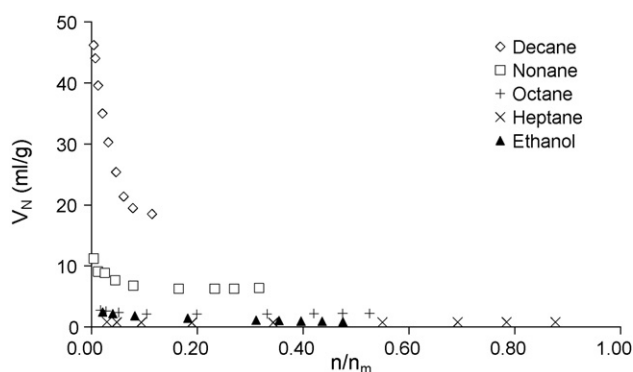

Fig. 7. Net retention volume against fractional surface coverage for untreated D-mannitol.
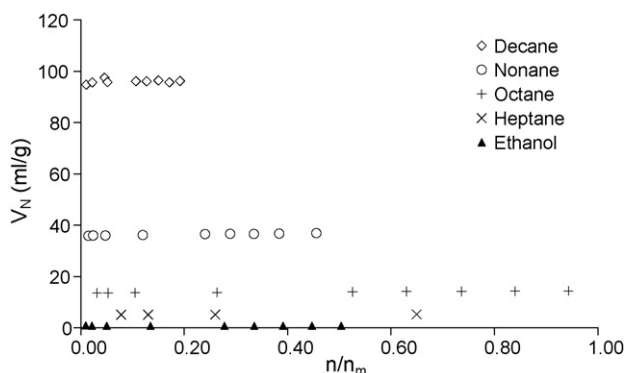
Fig. 8. Net retention volume against fractional surface coverage for silanised D-mannitol.

which the γ_{SV}^d of the solid is determined from a plot of $RT \ln V_N$ versus $a\left(\gamma_{LV}^d\right)^{1/2}$ where R is the universal gas constant, T is the temperature, a is the cross-sectional area of the probe molecule and γ_{LV}^d is the dispersive liquid–vapour surface tension of the probe. γ_{SV}^d values were calculated at surface coverages where the V_N for all alkane probes are present. The regression coefficient, R^2, obtained for each γ_{SV}^d value at each surface coverage was higher than 0.999. The resulting γ_{SV}^d distributions, displayed in Fig. 9, show that γ_{SV}^d varied from approximately 49 mJ/m^2 at 3% surface coverage down to approximately 40 mJ/m^2 at 12% surface coverage for the untreated sample, whilst γ_{SV}^d was relatively constant at approximately 34 mJ/m^2 for the silanised sample. The shift from a high and broad energy distribution for untreated D-mannitol to a low and almost homogeneous energy distribution for silanised D-mannitol is consistent, within experimental errors, with the anisotropic and isotropic γ_{SV}^d measured with contact angle on their respective single crystals as shown in Table 3. The γ_{SV}^d determined from both IGC and contact angle showed remarkably good agreement: the lowest γ_{SV}^d measured for the untreated sample corresponds to the lowest γ_{SV}^d measured on single crystals, i.e. facet (0 1 1), and γ_{SV}^d of facet (1 2 0) and (0 1 0) both fall within the range of the measured distribution. The approximately 5% of the untreated D-mannitol surface with a γ_{SV}^d of 45 mJ/m^2 or higher is likely to be due to the presence of higher energy indexed facets which were not accessible with macroscopic crystals grown in the current study. On the other hand, the silanised sample revealed a highly homogeneous surface in terms of surface energy as a result of chemical modification, and the surface energetics was consistent with homogeneity in surface chemistry.
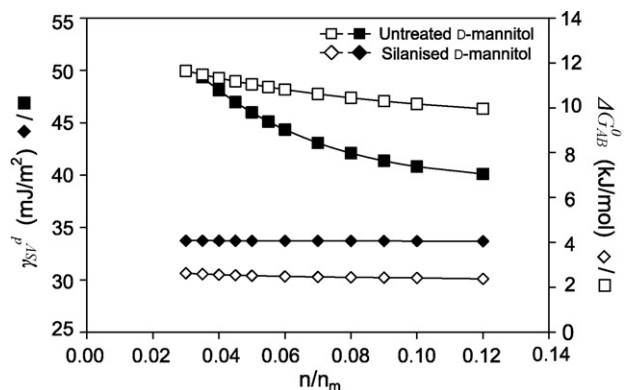

Fig. 9. γ_{SV}^d and ΔG_{AB}^0 (ethanol) distributions of untreated and silanised D-mannitol powders.

The distribution profiles of ΔG_{AB}^0 with ethanol as probe for untreated and silanised D-mannitol is also displayed in Fig. 9. In case of the untreated D-mannitol, the interaction between the vapour probe and hydroxyl groups on the surface of the sample is much stronger compared to the interaction between the probe and methyl groups on the silanised surface, and consequently the acid–base adsorption energy was much higher for the untreated sample than silanised sample. ΔG_{AB}^0 for untreated D-mannitol was up to 4.5 times more than the silanised sample at 3% surface coverage. Similar to their γ_{SV}^d profiles, the untreated powder sample exhibited heterogeneity in ΔG_{AB}^0 whereas the silanised sample showed high uniformity in surface chemistry. Though direct determination of the hydrophobicity ($\gamma_{SV}^d/\gamma_{SV}$) of the samples is not possible because γ_{SV}^d and ΔG_{AB}^0 have different units, the rank order of hydrophobicity of the two samples can be estimated by comparing their ΔG_{AB}^0 to γ_{SV}^d ratios, and it can be seen that the silanised sample was much hydrophobic compared to the untreated sample.

4. Conclusions

In the current work, the anisotropic surface energetics and wettability were validated for the first time on crystalline pharmaceutical excipient in the example of D-mannitol. The surface properties of crystalline excipients can be as important as their active counterpart in manufacturing and processing operations. The advancing contact angles for various crystal facets of β D-mannitol were found to be anisotropic. On those facets where hydroxyl functionality is in abundance, a significant hydrophilic behaviour was observed. The hydrophilicity order for β D-mannitol was determined as:

$$(0\,1\,1) > (1\,2\,0) > (0\,1\,0)$$

This was in good agreement with concentration of hydroxyl group distributions determined from XPS.

Crystal surfaces were found to become homogeneous after surface chemical induced modification by methyl groups. This was confirmed by both contact angle and IGC experiments. The measured γ_{SV}^d from contact angle on single crystals were in good agreement with the corresponding IGC γ_{SV}^d profile. The homogenous energy distribution for silanised mannitol can be attributed to the regularity in surface chemistry due to silanisation reaction which reduced γ_{SV}^d and ΔG_{AB}^0 of the surfaces, but did not induce bulk change in crystallographic structure. From both the measured contact angle polarity and IGC γ_{SV}^d and ΔG_{AB}^0 profiles, silanised mannitol samples were much more hydrophobic compared to untreated mannitol surfaces. Both contact angle and IGC were shown to be able to determine detailed surface energy distributions and distinguish energetic heterogeneity and homogeneity of pharmaceutical solids, reflecting the surface chemical environment.

References

Begat, P., Morton, D.A.V., Staniforth, J.N., Price, R., 2004. The cohesive–adhesive balances in dry powder inhaler formulations. I. Direct quantification by atomic force microscopy. Pharm. Res. 21, 1591–1597.

Buckton, G., Gill, H., 2007. The importance of surface energetics of powders for drug delivery and the establishment of inverse gas chromatography. Adv. Drug Deliv. Rev. 59, 1474–1479.

Burger, A., Henck, J., Hetz, S., Rollinger, J.M., Weissnicht, A.A., 2000. Energy/temperature diagram and compression behaviour of the polymorphs of D-mannitol. J. Pharm. Sci. 89, 457–468.

Charmas, B., Leboda, R., 2000. Effect of surface heterogeneity on adsorption on solid surfaces—application of inverse gas chromatography in the studies of energetic heterogeneity of adsorbents. J. Chromatogr. A 886, 133–152.

Davies, M., Brindley, A., Chen, X.Y., Marlow, M., Doughty, S.W., Shrubb, I., Roberts, C.J., 2005. Characterization of drug particle surface energetics and Young's modulus by atomic force microscopy and inverse gas chromatography. Pharm. Res. 22, 1158–1166.

Grimsey, I.M., Sunkersett, M., Osborn, J.C., York, P., Rowe, R.C., 1999. Interpretation of the differences in the surface energetics of two optical forms of mannitol by inverse gas chromatography and molecular modelling. Int. J. Pharm. 191, 43–50.

Heng, J.Y.Y., Bismarck, A., Lee, A.F., Wilson, K., Williams, D.R., 2006a. Anisotropic surface energetics and wettability of macroscopic form I paracetamol crystals. Langmuir 22, 2760–2769.

Heng, J.Y.Y., Bismarck, A., Williams, D.R., 2006b. Anisotropic surface chemistry of crystalline pharmaceutical solids. AAPS PharmSci 7 Article 84, E1–E9.

Heng, J.Y.Y., Thielmann, F., Williams, D.R., 2006c. The effects of milling on the surface properties of form I paracetamol crystals. Pharm. Res. 23, 1918–1927.

Heng, J.Y.Y., Williams, D.R., 2006. Wettability of paracetamol polymorphic forms I and II. Langmuir 22, 6905–6909.

Ho, R., Heng, J.Y.Y., Dilworth, S.E., Williams, D.R., 2008. Wetting behaviour of ibuprofen racemate surfaces. J. Adhes. 84, 483–501.

Jaroniec, M., Madey, R., 1988. Physical Adsorption on Heterogeneous Solids. Elsevier, Amsterdam.

Kaminsky, W., Glazer, A.M., 1997. Crystal optics of D-mannitol, $C_6H_{14}O_6$: crystal growth, structure, basic physical properties, birefringence, optical activity, Faraday effect, electro-optic effects and model calculations. Z. Kristallogr. 212, 283–296.

Li, Q., Rudolph, V., Weigl, B., Earl, A., 2004. Interparticle van der Waals force in powder flowability and compactibility. Int. J. Pharm. 280, 77–93.

Newell, H.E., Buckton, G., 2004. Inverse gas chromatography: investigating whether the technique preferentially probes high energy sites for mixtures of crystalline and amorphous lactose. Pharm. Res. 21, 1440–1444.

Newell, H.E., Buckton, G., Butler, D.A., Thielmann, F., Williams, D.R., 2001. The use of inverse phase gas chromatography to measure the surface energy of crystalline, amorphous, and recently milled lactose. Pharm. Res. 18, 662–666.

Owens, D.K., Wendt, R.C., 1969. Estimation of the surface free energy of polymers. J. Appl. Polym. Sci. 13, 1741–1747.

Pifferi, G., Santoro, P., Pedrani, M., 1999. Quality and functionality of excipients. Farmaco 54, 1–14.

Saxena, A., Kendrick, J., Grimsey, I., Mackin, L., 2007. Application of molecular modelling to determine the surface energy of mannitol. Int. J. Pharm. 343, 173–180.

Schultz, J., Lavielle, L., Martin, C., 1987. The role of the interface in carbon fibre–epoxy composites. J. Adhes. 23, 45–60.

Thielmann, F., Burnett, D.J., Heng, J.Y.Y., 2007. Determination of the surface energy distributions of different processed lactose. Drug Dev. Ind. Pharm. 33, 1240–1253.

Thielmann, F., Naderi, M., Ansari, M.A., Stepanek, F., 2008. The effect of primary particle surface energy on agglomeration rate in fluidised bed wet granulation. Powder Technol. 181, 160–168.

Walter-Levy, L., 1968. Crystalline varieties of D-mannitol. Comptes Rendus Hebdomadaries Des Seances De L Academie Des Sciences Serie C 267, 1779–1782.

Yoshinari, T., Forbes, R.T., York, P., Kawashima, Y., 2002. Moisture induced polymorphic transition of mannitol and its morphological transformation. Int. J. Pharm. 247, 69–77.

Zhang, D., Flory, J.H., Panmai, S., Batra, U., Kaufman, M.J., 2002. Wettability of pharmaceutical solids: its measurement and influence on wet granulation. Colloids Surf. A 206, 547–554.